

The Galactic Wind Haze and its γ -spectrum

Nayantara Gupta¹, Biman B. Nath¹, Peter L. Biermann^{2,3,4,5,6}, Eun -Suk Seo⁷, Todor Stanev⁸, Julia Becker Tjus⁹

¹ Raman Research Institute, Sadashiva Nagar, Bangalore 560080, India

² MPI for Radioastronomy, Bonn, Germany

³ Dept. Physics., Karlsruher Institut für Technologie, Karlsruhe, Germany

⁴ Dept. of Phys. & Astr., Univ. of Alabama, Tuscaloosa, AL, USA

⁵ Dept. of Phys., Univ. of Alabama at Huntsville, AL, USA

⁶ Dept. of Phys. & Astron., Univ. of Bonn, Germany

⁷ Dept. of Physics, Univ. of Maryland, College Park, MD, USA

⁸ Bartol Research Inst., Univ. of Delaware, Newark, DE, USA

⁹ Institut für theoretische Physik, Plasma-Astroteilchenphysik, Ruhr-Universität Bochum, D-44780, Bochum, Germany

21 January 2013

ABSTRACT

The spectrum observed by Fermi-LAT from the Galactic centre region shows a gamma ray feature near 130 GeV, that in some analyses appears as a possible line. We discuss the possibility that this gamma ray feature has a cosmic ray origin. We argue that the cosmic ray electrons steepen near 1 TeV from E^{-3} to about $E^{-4.2}$, and are all secondary derived from the knee-feature of normal cosmic rays. We argue that the observed feature at ~ 130 GeV could essentially be a noise feature on top of a sharp turn-off in the γ ray spectrum at ~ 130 GeV. This match suggests that the knee of normal cosmic rays is the same everywhere in the Galaxy. We suggest that it follows that all supernovae contributing give the same cosmic ray spectrum, with the knee feature given by common stellar properties; in fact, this is consistent with the supernova theory proposed by Bisnovatyi-Kogan (1970), a magneto-rotational mechanism: Massive stars converge to common properties in terms of rotation and magnetic fields just before they explode.

Key words: stars:winds,outflows; gamma-rays:galaxies

1 INTRODUCTION

Fermi-LAT has revealed many interesting phenomena in the gamma ray sky. The Fermi bubbles have been observed extending up to 10 kpc upwards and below from the Galactic Center (GC) (Su et al. 2010) in the 1-100 GeV energy range. More recently a Fermi group has reported the detection of GeV line emission from the Galactic centre region (Ackermann et al. 2012). The diffuse gamma ray data taken by Fermi-LAT show a weak line or lines from 1.5° west of the Galactic Center (GC) (Su & Finkbeiner 2012). The observational features of the line like structure are not yet clear. More sensitive detectors are needed to confirm and resolve this structure (Li & Yuan 2012) and then it would be possible to know whether these are lines and dark matter signatures or some astrophysical broadband effect. Su & Finkbeiner (2012) have interpreted the observational data as a single spectral line at 127 ± 2 GeV or a pair of lines at 110.8 ± 4.4 GeV and 128.8 ± 2.7 GeV giving a slightly better fit. The analysis of the Fermi-LAT data by Cohen et al. (2012) prefers a single line either at 130 GeV or

145 GeV. The line emission has been explained earlier with dark matter annihilations (Bringmann et al. 2012, Weniger 2012, Tempel et al. 2012, Kyae & Park 2012, Lee et al. 2012, Rajaraman et al. 2012, Buckley & Hooper 2012, Su & Finkbeiner 2012, Hea & Kim 2012, Yang et al. 2012).

Cosmic rays may also explain the gamma ray feature at 130 GeV. It has been suggested that a break in the gamma ray spectrum of the Fermi Bubbles may appear as an excess at 130 GeV (Profumo & Linden 2012).

The interstellar total radiation field has been calculated by Moskalenko et al. (2006) as a function of the Galactocentric radius, taking into account the emission by stars of different types and the scattering, absorption and re-emission of starlight by dust grains. It has distinct peaks and the photon density is maximum near $50-100\mu\text{m}$ and in the next peak near $1000\mu\text{m}$. The intensity of the radiation field near the GC region is expected to be much higher than its locally observed value. In the present work we show that the 130 GeV feature could be due to the Inverse Compton scattering of the infrared photons of wavelength $50\mu\text{m}$ with the cosmic ray electrons of energy 1 TeV where the electron spectrum

steepens from E^{-3} to about $E^{-4.2}$. We then show how this fits into a broader interpretation of recent cosmic ray data, and conclude that the underlying cosmic ray electron spectrum near TeV energies very likely is the same in the GC region and near us. This strongly suggests that these electrons are secondary from spallation of cosmic ray nuclei near the knee energies, of about a few PeV; the cosmic ray nuclei spectrum then also has to be essentially the same at high energy in the Galactic centre region and near us, and quite specifically show the knee feature at the same energy.

2 STAR FORMATION AT GALACTIC CENTRE AND FERMI BUBBLES

Multi-wavelength observations have revealed surprising phenomena near the core of our Galaxy. The Fermi-LAT gamma ray detector has observed two large bubbles symmetrically located below and above the centre of our Galaxy. The bubbles extend up to 10 kpc above and below the Galactic plane with a width of 40° .

More interestingly, the WMAP (Jarosik et al. 2011) and Planck (Ade et al. 2012) haze is located within the northern bubble sharing the same edges and the ROSAT soft X-ray maps (Snowden et al. 1997) are in the circumference of the bubbles. These observational correlations suggest a common origin of these emissions. The gamma ray energy flux in the energy range of 1–100 GeV from Fermi Bubbles is $E_\gamma^2 dN(E_\gamma)/dE_\gamma = 3 \times 10^{-7}$ GeV cm $^{-2}$ s $^{-1}$ sr $^{-1}$ and the solid angle subtended is 0.808 sr (Su et al. 2010).

This gamma ray emission has been explained as a result of cosmic ray protons interacting with protons in the medium (Crocker & Aharonian 2011) which leads to the production of charged and neutral pions. In this scenario if the cosmic ray protons are trapped for timescales of 10^{10} years, their energy partially going to the high energy gamma rays produced from decaying neutral pions can explain the observations by Fermi-LAT.

A more detailed discussion on mass and energy flows through the Galactic centre and into the Fermi Bubbles is given in Crocker (2012). Within a single-zone model it is shown that the star formation in the Galactic centre can sustain the energetics of the system and it explains the observed non-thermal emissions.

Cheng et al. (2011) have interpreted the observational features near the core of our Galaxy as a result of periodic star capture processes by the galactic supermassive black hole $SgrA^*$. Hot plasma wind is injected into the halo which subsequently heats up the halo gas. The hot gas produces thermal X-rays. The periodic injection of hot plasma also produces shocks and accelerate the electrons to TeV energy. Their synchrotron and Inverse Compton emission may explain the observed radio and gamma ray emission from the central part of our Galaxy.

The bubbles are also explained as evidence of possible AGN jet activity in our Galaxy (Guo et al. 2011), last quasar outburst (Zubovas et al. 2011) and collimation of a wide angle outflow from $SgrA^*$ (Zubovas et al. 2012) by the Central Molecular Zone.

The bubbles could be the result from second order Fermi acceleration of electrons by plasma wave turbulence through out the entire volume of the bubbles (Mertsch & Sarkar

2011). The authors of this paper have explained the observed gamma ray emission with Inverse Compton losses of the hard spectrum of electrons resulting from second order Fermi acceleration.

The magnetic field structure in the northern Fermi Bubble has been explored with polarized microwave emission (Jones et al. 2012). Their study reveals that the magnetic field lines in the northern Bubble's eastern wall and Galactic centre Spur are almost perpendicular to their extensions above the Galactic plane.

We consider the case of a bubble being produced by the action of star formation in the Galactic centre region. Recent observations deduce a star formation rate of ~ 0.04 – 0.08 M $_\odot$ yr $^{-1}$, lasting about ~ 1 – 10 Myr (Yousef-Zadeh et al 2009; Immer et al 2012). The combined rate of momentum deposition from supernovae and stellar winds is then estimated to be $F \sim 5 \times 10^{33} (SFR/1 M_\odot/\text{yr}) \sim 2.5 \times 10^{32}$ dyne for a $SFR \sim 0.05$ M $_\odot$ yr $^{-1}$ (Leitherer et al 1999). There is also likely to be a component of pressure from cosmic rays driving this wind (Everett et al 2008; Uhlig et al 2012). If we consider a bubble blown by the combined momentum injection traversing a distance of $L \sim 10$ kpc in 15 Myr then the total energy deposited is $\sim F \times L \sim 7.7 \times 10^{54}$ erg. A fraction $\sim 15\%$ of this energy going to cosmic rays would produce a cosmic ray energy budget of $\sim 10^{54}$ erg, consistent with the estimate of Su et al. (2010). The implied energy density in a bubble of radius ~ 5 kpc is $\sim 1.4 \times 10^{-11}$ erg cm $^{-3}$, and the equipartition magnetic field is estimated to be $\sim 4 \mu\text{G}$, consistent with the recent measurement of magnetic field in the bubble by Carretti et al. (2013).

3 THE COSMIC RAY SPECTRUM IN THE GALACTIC CENTER REGION

The spectrum of cosmic rays is determined by their injection spectrum, their transport processes, and their losses. In a series of papers from 1993 (Biermann 1993; Biermann & Cassinelli 1993; Biermann & Strom 1993; Stanev et al. 1993) it has been proposed, that the injection of Galactic cosmic rays can be divided into two main source classes, one due to explosions into the interstellar medium, and one due to explosions into the predecessor stellar wind. For the ISM-SN-CRs the prediction had been a spectrum of $E^{-2.75 \pm 0.04}$ after taking into account transport processes (with a Kolmogorov spectrum), $E^{-2.67 \pm 0.04}$ for wind-SN-CRs below the knee, and the spectrum of $E^{-3.07 \pm 0.14}$ above the knee. The most recent fits to data give spectral index -3.08 beyond the knee (Biermann et al. 2003, Abbasi et al. 2012a, 2012b, Biermann & de Souza 2012).

The knee energy scales with the charge of the nucleus, and is about 600 Z TeV, with a large uncertainty in its original prediction. The wind-Supernovae also have a polar cap component with an injection spectrum of E^{-2} and a sharp cutoff at the knee-energy due to a spatial limit in the acceleration region. The final cutoff for ISM-SN-CRs had been predicted to be around 100 Z TeV, and for wind-SN-CRs at about 100 Z PeV; these predictions had been summarized in Biermann (1994), and Biermann et al. (2001). Since 2009 a series of tests have been possible that checked on the predictions, the CR-electron and CR-positron spectra (Biermann et al. 2009), the WMAP haze and 511 keV emission line

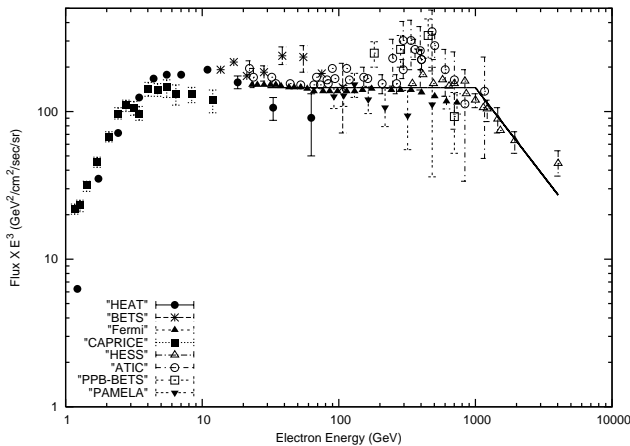


Figure 1. Observed electron spectrum near the earth proportional to E^{-3} and $E^{-4.2}$ below and above the break at 1 TeV respectively.

(Biermann et al. 2010a), the spectra of the various elements constituting the ISM and the wind components (Biermann et al. 2010b), and the different spallation histories for ISM-SN-CRs and wind-SN-CRs (Nath et al. 2012), with a low interaction column for ISM-SN-CRs and a high column for the wind-SN-CRs. The spectrum of the cosmic rays beyond the knee was tested in Biermann & de Souza (2012). These predictions have also been used in explanations of the ultrahigh energy cosmic rays (Gopal-Krishna et al. 2010, Biermann & de Souza 2012), invoking a shift of the normal cosmic rays by a one-cycle relativistic shock following Gallant & Achterberg (1999), and Achterberg et al. (2001) in the neighboring radio galaxy Cen A. The Fermi data of the Galactic Center region provide another test for these proposals.

Here we address the possibility that there is a sharp spectral feature at 130 GeV in the region of the Galactic Center. For this we need to summarize the properties of the relevant cosmic ray electrons. The polar cap component of $E^{-7/3}$ in observer frame has a sharp cut-off at the knee energy, while the 4π component goes from $E^{-8/3}$ to about $E^{-3.2}$ at exactly the same energy. Pitch angle scattering and smoothing in the spallation production of the secondary leptons will modify this original spectral shape. After propagation the polar cap component of electrons from wind-SNe steepens to $E^{-2-1/3}$ due to diffusion losses and at higher energy E^{-2-1} due to synchrotron and Inverse Compton losses.

Interestingly, a break near 1 TeV in the electron spectrum has been observed near Earth (Biermann et al. 2009) and it is expected to be present also near the Galactic centre region.

The knee near 4 PeV in the high energy cosmic ray spectrum can be correlated with the break in the electron spectrum at 1 TeV. Near the knee the cosmic rays are mostly He and heavier nuclei. The Lorentz factor of the heavy nuclei at the knee $\gamma_{knee} = Z/A\gamma_p$, where γ_p is the Lorentz factor of the protons. Z/A is nearly 1/2 for all heavy nuclei. We therefore find $\gamma_{knee} = 2 \times 10^6$, which is also the Lorentz factor of the 1 TeV cosmic ray electrons at the break. The secondary electrons are perhaps produced in nuclear de-excitation following energetic particle interactions (Ramaty et al. 1979)

and as a result their Lorentz factors are approximately the same as that of the parent nuclei.

The cosmic ray electron spectrum observed near Earth is shown in Figure 1: in the energy range of 100 GeV to 4 TeV. The solid line shows the electron spectrum proportional to E^{-3} and $E^{-4.2}$ below and above the break at 1 TeV respectively. We will show below that if the steepening from E^{-3} to $E^{-4.2}$ is at 1 TeV then the Inverse Compton scattering of the infrared background photons by the electrons at the break energy can explain the 130 GeV line feature in the γ ray spectrum near GC. This requires the cosmic ray electron spectrum around TeV energies to be essentially the same in shape near the Galactic Center as near Earth.

4 130 GEV FEATURE EMISSION NEAR GC

The interstellar radiation (IR) field has been estimated (Moskalenko et al. 2006) at different distances from the GC. The intensity of the field is highest at GC and decreases with distance from GC. The polar cap component of the electron spectrum (in the loss dominant case) as observed near the Earth is

$$\frac{dN_e}{d\gamma_e} = 23.55 \times 10^{-6} \gamma_e^{-3} \text{ cm}^{-3} \quad (1)$$

We assume near the Galactic centre region the electron flux is $\eta > 1$ times the flux observed near the Earth. The γ ray flux produced by Inverse Compton scattering of infrared photons near GC region is calculated.

$$E_\gamma^2 \frac{dN(E_\gamma)}{dE_\gamma} = E_\gamma \frac{Vol}{4\pi D_{GC}^2} \frac{dE_{IC}}{dVdE_\gamma dt} \frac{1}{\Delta\Omega} \quad (2)$$

We are considering a region with $-15^\circ \leq b \leq 15^\circ$ and $-20^\circ \leq l \leq 20^\circ$ near the Galactic centre, which is similar to the region 3 given in Fig.1. of Weniger 2012. The solid angle subtended by this region to the observer on the Earth is $\Delta\Omega = 2 \times \int_0^{20^\circ} d\phi \int_{90^\circ-15^\circ}^{90^\circ} \sin\theta d\theta = 0.36 \text{ sr}$, where $\phi = l$ and $\theta = 90^\circ - b$. The distance to GC from the Earth is $D_{GC} = 7.5 \text{ kpc}$ (Nishiyama et al. 2006, Eisenhauer et al. 2005) which gives $4\pi D_{GC}^2 = 10^{45.8} \text{ cm}^2$.

The power emitted per unit volume, per unit energy and per unit time by the gamma rays produced in Inverse Compton scattering is expressed as $\frac{dE_{IC}}{dVdE_\gamma dt}$. The electron spectral index $p = 3$ gives gamma ray spectral index $(p-1)/2+1 = 2$, $\frac{dN(E_\gamma)}{dE_\gamma} \propto E_\gamma^{-2}$. The expression for power emitted in Inverse Compton scattering by electrons is (Rybicki & Lightman 1979)

$$\frac{dE_{IC}}{dVdE_\gamma dt} = 23.55 \times 10^{-6} \eta c \pi r_0^2 A_p E_\gamma^{-1} \int \epsilon v(\epsilon) d\epsilon \quad (3)$$

where $v(\epsilon)$ is the low energy photon density per unit energy ϵ . The value of the constant A_p for $p = 3$ is $16/9$, the classical electron radius $r_0 = 2.817 \times 10^{-13} \text{ cm}$ and c is the speed of light. We have taken $\eta \times Vol/(10^{64.6} \text{ cm}^3) \sim 10$, where η is taken to be of order unity in order to take into account the possible variation in CR flux in the galactic centre area, and also the uncertainty in our knowledge of the volume. After taking angular average the electron Lorentz factor (γ_e), target photon energy (ϵ) and scattered photon energy (E_γ) are related as $4/3\gamma_e^2\epsilon = E_\gamma$. Thus the electrons of energy 1 TeV Inverse Compton scatter the IR photons of energy 0.024 eV

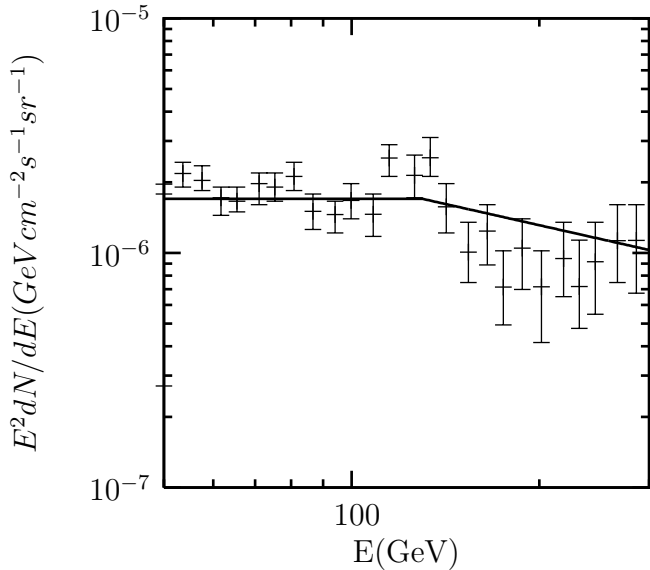


Figure 2. Gamma ray data with error bars from Reg3 in Fig.1 of Weniger 2012, solid line shows spectral shape with E^{-2} and $E^{-2.6}$ below and above 130 GeV respectively.

which corresponds to wavelength $50\mu\text{m}$ and 130 GeV γ rays are produced.

The IR background has several peaks as shown in Figure 1 of Moskalenko et al. (2006). The IR photon density at the peak near 0.024–0.012 eV is higher than the densities at the higher energy peaks near 1.2 eV and 0.12 eV. It is comparable to the photon density at the next lower energy peak at 0.0012 eV. The IR photons of energy 0.024 eV are mostly contributing to the gamma ray spectrum near 130 GeV. The lower energy IR photons produce gamma rays of the same energy by Inverse Compton scattering off higher energy electrons. As the electron spectrum steepens beyond 1 TeV the contribution to the gamma ray flux at 130 GeV from the lower energy IR photons near 0.0012 eV is not significant. We have parametrized the IR peak near 0.024 eV as a delta function at that energy. We have used IR photon density $1/(0.024)^2 \text{ eV}^{-1} \text{ cm}^{-3}$ in our calculations (Moskalenko et al. 2006). The flux of the gamma rays is calculated using eqn(2), eqn(3) and compared with the observed flux in Figure 2 of this paper.

The calculated gamma ray spectrum is proportional to $E^{-2.6}$ above 130 GeV. The sharp decrease in photon flux near 130 GeV due to the change in the spectral index of the electron spectrum has perhaps been observed as a line-like feature in the Fermi LAT data.

5 DISCUSSIONS

The gamma ray emission observed by Fermi-LAT near the GC region has been explained as Inverse Compton emission of cosmic ray electrons. The IR background photons in this region are Inverse Compton scattered off the cosmic ray electrons. The Galactic wind driven by star formation in the GC region and the emitted cosmic rays supplies the energy of

$\sim 10^{54}$ erg to the bubbles of gamma rays. The break in the bubble's spectrum due to the break in the spectrum of the cosmic ray electrons appears as a line near 130 GeV.

The intensity of gamma rays from the bubbles does not show any significant variation with distance from GC. This may be understood as follows: a) The gamma ray intensity of Fermi Bubbles depends on the intensity of the background IR radiation field and the density of the cosmic ray electrons. The IR radiation is essentially constant initially up into the halo as long as the lateral scale of the emitting region is larger than the distance above the disk. b) The density of the cosmic ray electrons is inversely proportional to the cross-section of the flow. If the initial flow is straight up, then the density changes only slowly and adiabatic losses may be weak. Moreover, re-acceleration by weak shocks (eqn. 2.45 in Drury 1983) may keep the spectral shape of the cosmic ray electrons intact but sharpen the kink in the spectrum. c) What we observe is a line of sight integral, so even a decrease of the IR radiation field weaker or similar to r^{-1} would be compensated in the integral for a straight initial flow up/down. Taken together this allows to understand the constancy of the emission.

Fermi-LAT has also observed emission of gamma rays in 1–100 GeV band in the star forming region of Cygnus X (Ackermann et al. 2011). The observed gamma ray spectrum is proportional to E^{-2} . The polar cap component of cosmic rays at the source is proportional to E^{-2} and it gives secondary pions in hadronic interactions. The neutral pions subsequently decay to gamma rays. Thus the gamma ray spectrum observed from Cygnus X might have originated in hadronic interactions of the polar cap component of cosmic rays. IC emission spectrum of secondary electrons in this case would be proportional to $E^{-3/2}$ and inconsistent with the observed spectrum E^{-2} .

The direct observations of the cosmic ray electron spectrum near the Earth give us the loss-dominant spectrum of the cosmic ray electron spectrum in our neighborhood, and the gamma-ray observations give us that spectrum in the Galactic Center region. It is very interesting that the derived spectral shape is the same.

It is possible to relate the knee in the very energy cosmic ray spectrum with the break in the cosmic ray electron spectrum. Cosmic ray interactions and subsequent nuclear de-excitation leads to the production of the secondary electrons, as the cosmic ray parent nuclei and secondary electrons have the same Lorentz factor. This implies that the cosmic ray knee is at the same energy in terms of E/Z everywhere in the Galaxy as the break energy in the electron spectrum is same in different regions of the Galaxy, as predicted from a theory, that attributes this kink to the original stars. This derives from the fact, that in different parts of the Galaxy very different stars contribute to the kink feature of cosmic rays, the knee, and in each location very many stars contribute. So to have a clear feature at all, and then to have that feature the same in different parts of the Galaxy puts very strong constraints on the exploding stars: they must all be asymptotically very similar at the point of explosion.

We need to ask, whether any other mechanism could produce such a kink in the cosmic ray spectrum, and also give a break energy which is the same everywhere in the Galaxy: First we may consider the possibility that OB superbubbles produce the cosmic ray component giving the knee;

in such a theory a curvature upwards and below the energy of the knee would be consistent with arguments on shock structure (e.g. Drury 2011); One might speculate that it could also produce a knee from a characteristic length scale of the super-bubble. However, it is hard to see how this critical length scale can be the same everywhere in the Galaxy. Second, we can generalize this argument to the transport in the Galaxy, and the escape from the Galaxy. However, as is well known, this possibility would give a much larger cosmic ray anisotropy in arrival directions than what has been observed, and so is also wrought with difficulties (e.g. Biermann 1993, and the references mentioned there).

So, it appears that the original exploding stars are required to explain this kink, called the knee. This has actually been predicted (Biermann 1993), and is based on the magneto-rotational mechanism for the explosions of very massive stars proposed by Bisnovatyi-Kogan (1970), and worked out in much more detail by Ardeljan et al. (2005), Moiseenko et al. (2006), Bisnovatyi-Kogan & Moiseenko (2007) and others. This mechanism connects the rotation of the core of the star with the magnetic fields, just as is required to explain a constant knee E/Z scale (Biermann 1993).

We can also make further tests of the proposal. If the E^{-3} segment of the cosmic ray electron spectrum is secondary, then the upturn should be connected to the parallel upturn in the positrons (e.g. Biermann et al. 2009, now Adriani et al. 2011); in fact this is consistent.

The cosmic ray electrons are also emitting synchrotron photons which have been observed in the Planck spectrum (Ade et al. 2012). One zone compatible with radio spectrum ν^{-1} due to the electron spectrum E^{-3} in the loss limit and another with a spectrum compatible with $\nu^{-2/3}$ due to the electron spectrum $E^{-7/3}$ in the diffusion limit are expected to be observed by Planck. A ring may be present at the transition region between the outer zone of high frequency radio spectrum proportional to ν^{-1} and inner zone where it is proportional to $\nu^{-2/3}$. Perhaps due to ignoring the ring region the Planck data is at present consistent with a slightly steeper spectrum in the outer zone and a flatter spectrum in the inner zone.

It is also expected that there should be many wind-SN-remnants with a spectrum of $E^{-7/3}$ at lower gamma ray energies, and E^{-2} at higher energies.

6 CONCLUSIONS

In this work we propose an explanation of the 130 GeV line-like feature appearing in the GC gamma ray emission in the Fermi data: The idea is that this is just a noise feature on top of a sharp kink in the underlying continuum. The continuum is explained as Inverse Compton emission of the FIR radiation field by secondary cosmic electrons/positrons produced in spallation of cosmic ray nuclei at the knee.

We realize that this implies that the cosmic ray electron spectrum has the same shape at high energy in the GC region as near to Earth in the Galaxy. This implies then in our concept that the cosmic ray particles themselves have the same knee energy through out the Galaxy. This in turn supports an origin of this feature in the original supernova

explosions, which in turn supports the magneto-rotational mechanism proposed by Bisnovatyi-Kogan (1970).

If all this is true, we have identified a common quantitative feature of all very massive stars in the final stage just before they blow up, connecting rotation and magnetic fields.

7 ACKNOWLEDGEMENTS

PLB acknowledges discussions about this and related topics with W. Cui, R. Diehl, J. Finley, A. Haungs, A. Meli, M. Roth, D. Ryu, V. de Souza, and many others. Support for E.-S.S. comes from NASA grant NNX09AC14G and for T.S. comes from DOE grant UD-FG02-91ER40626.

REFERENCES

- Abbasi, R. et al. 2012a, arXiv:1202.3039
- Abbasi, R. et al. 2012b, arXiv:1207.3455
- Achterberg, A., Gallant, Y. A., Kirk, J. G., Guthmann, A. W. 2001, *MNRAS*, 328, 393
- Ackermann, M. et al. 2012, *Phys. Rev. D*, 86, 022002
- Ackermann, M. et al. 2011, *Science*, 334, 1103
- Ade, P. A. R. et al. 2012, arXiv:1208.5483
- Adriani, O. et al. 2011, *Phys. Rev. Lett.*, 106, 201101
- Ardeljan, N. V., Bisnovatyi-Kogan, G. S., Moiseenko, S. G., 2005, *MNRAS*, 359, 333
- Beringer, J. et al. (Particle Data Group), *Phys. Rev. D*, 86, 010001 (2012)
- Beck, R., Brandenburg, A., Moss, D., Shukurov, A., Sokoloff, D. 1996, *ARA&A*, 34, 155
- Biermann, P.L. 1993, *A&A*, 271, 649 (CR-I)
- Biermann, P.L., & Cassinelli, J.P. 1993, *A&A*, 277, 691 (CR-II)
- Biermann, P.L., & Strom, R.G. 1993, *A&A*, 275, 659, CR-III
- Biermann, P.L. (1994), 23rd International Conference on Cosmic Rays, in Proc. "Invited, Rapporteur and Highlight papers"; Eds. D. A. Leahy et al., World Scientific, Singapore, 1994, p. 45
- Biermann, P.L., Langer, N., Seo, E. S., Stanev, T. 2001, *A&A*, 369, 269
- P. L. Biermann, S. Moiseenko, S. Ter-Antonyan, & A. Vasile, Invited review at the 9th course of the Chalonge School on Astrofundamental Physics: "The Early Universe and The Cosmic Microwave Background: Theory and Observations"; Eds. N.G. Sanchez & Y.N. Parijski, Kluwer, p. 489 - 516 (2003), astro-ph/0302201
- Biermann, P. L., Becker, J. K., Meli, A., Rhode, W., Seo, E. S., Stanev, T. 2009, *Phys. Rev. Lett.*, 103, 061101
- Biermann, P.L., Becker, J. K., Caceres, G., Meli, A., Seo, E. S., Stanev, T. 2010, *ApJ*, 710, L53
- Biermann, P.L., Becker, J. K., Dreyer, J., Meli, A., Seo, E. S., Stanev, T. 2010b, *ApJ*, 725, 184
- Biermann, P.L., & de Souza, V. 2012, *ApJ*, 746, 72
- Bisnovatyi-Kogan, G. S., *Astron. Zh.*, 47, 813 (1970); transl. *Sov. Astron.*, 14, 652 (1971)
- Bisnovatyi-Kogan, G. S.; Moiseenko, S. G., 2007, *Astronomical and Astrophysical Transactions*, 26, 71

Bringmann, T., Huang, X., Ibarra, A., Vogl, S., Weniger, C. 2012, *JCAP*, 07, 054

Buckley, M. R. & Hooper, D. 2012, *Phys. Rev. D*, 86, 043524

Carretti E. et al. 2013, *Nature*, in press (arXiv: 1301.0512)

Cheng, K. S. et al., 2011, *ApJ*, 731, L17

Crocker, R. M. 2012, *MNRAS*, 423, 3512

Crocker, R. M. & Aharonian, F., 2011, *Phys. Rev. Lett*, 106, 101102

Drury, L. O'C. 1983, *Rep. Pro. Phys.*, 46, 973

Drury, L. O'C., *MNRAS*, 415, 1807 (2011)

Eisenhauer, F. et al. 2005, *ApJ*, 628, 246

Everett, J. E., Zweibel, E. G., Benjamin, R. A., McCammon, D., Rocks, L., Gallagher III, J. S. 2008, *ApJ*, 674, 258

Gallant, Y.-A., Achterberg, A. 1999, *MNRAS*, 305, L6

Gopal-Krishna, Biermann, P. L., de Souza, V. & Wiita, P. J. 2010, *ApJ*, 720, L155

Guo, F. & Mathews, W. G., 2011, arXiv:1103.0055

Heo, J. H. & Kim, C. S. 2012, arXiv:1207.1341

Immer, K., Schuller, F., Omont, A., Menten, K. M. 2012, *A&A*, 537, 121

Jarosik, N., Bennett, C. L., Dunkley, J. et al. 2011, *ApJ*, 192, 14

Jones, D. I., Crocker, R. M., Reich, W., Ott, J., Aharonian, F. A. 2012, *ApJ*, 747, L12

Kyae, B. & Park, J.-C. 2012, arXiv:1205.4151

Lee, H. M., Park, M. & Park, Wan-II 2012, arXiv:1205.4675

Leitherer, C. et al. 1999, *ApJS*, 123, 3

Li, Y. & Yuan, Q. 2012, *Phys. Lett.B*, 715, 35

Mertsch, P. & Sarkar, S., 2011, *Phys. Rev. Lett*, 107, 091101

Moiseenko, S. G., Bisnovatyi-Kogan, G. S.; Ardeljan, N. V. 2006, *MNRAS*, 370, 501

Moskalenko, I. V., Porter, T. A., Strong, A. W. 2006, *ApJ*, 640, 155

Nath, B., Gupta, N. & Biermann, P. L. 2012, *MNRAS*, 425, L86

Nishiyama, S. et al. 2006, *ApJ*, 647, 1093

Profumo, S. & Linden, T. 2012, *JCAP*, 07, 011

Rajaraman, A., Tait, T. & Whiteson D. 2012, arXiv:1205.4723

Ramaty R., Kozlovsky B. & Lingenfelter R. E. 1979, *ApJS*, 40, 487

Rybicki, G. B. & Lightman, A. P., *Radiative Processes in Astrophysics*, Wiley - Interscience publications (1979)

Snowden, S. L. et al. 1997, *ApJ*, 485, 125

Stanev, T., Gaisser, T.K., Biermann, P.L. 1993, *A&A*, 274, 902, CR-IV

Su, M., Slatyer, T. R., Finkbeiner, D. P. 2010, *ApJ*, 724, 1044

Su, M. & Finkbeiner, D. P. 2012, arXiv:1206.1616

Tempel, E., Hektor, A. and Raidal, M. 2012, arXiv:1205.1045

Uhlig, M., Pfrommer, C., Sharma, M., Nath, B. B., Ensslin, T., Springel, V. 2012, *MNRAS*, 423, 2374

Weniger, C. 2012, *JCAP*, 08, 007

Yang, R.-Z., Yuan, Q., Feng, L., Fan, Y.-Z., Chang, J. 2012, *Phys. Lett.B*, 715, 285

Yusef-Zadeh, F. et al. 2009, *ApJ*, 702, 178

Zubovas, K., King, A. R. & Nayakshin, S., 2011, *MNRAS*, 415, L21

Zubovas, K. & Nayaksin, S., 2012, *MNRAS*, 421, 1315